






PAPER

[View Article Online](#)
[View Journal](#) | [View Issue](#)

Cite this: *J. Mater. Chem. C*, 2022, **10**, 5466

Protein-based (bio)materials: a way toward high-performance graphene enzymatic biosensors†

Alessandro Silvestri, ^a Faxing Wang, ^b Xinliang Feng, ^b
Aitziber L. Cortajarena ^{a,c} and Maurizio Prato ^{a,b,c,d}

Enzymes are ideal receptors for biosensors since they offer excellent selectivity and high catalytic activity. However, once removed from their native environment, enzymes present a short lifespan determining a huge drawback for their application in bio-analytical systems. The use of appropriate immobilization matrices is an effective strategy to preserve enzymatic activity. In this work, an enzymatic amperometric biosensor is designed by entrapping lactate oxidase into a protein-based immobilization matrix, formed by the self-assembly of engineered repeat proteins. Electrochemically exfoliated graphene, functionalized with cobalt phthalocyanine, is employed as electroactive material and transducer of the sensor. Due to the extraordinary enzymatic stabilization provided by the engineered protein film, the device sensitivity is preserved for more than 6 months at room temperature. Furthermore, the presented biosensor can detect lactate with outstanding performance in terms of sensitivity, repeatability, and reproducibility.

Received 3rd February 2022,
Accepted 26th February 2022

DOI: 10.1039/d2tc00483f

rsc.li/materials-c

Introduction

Almost 60 years have passed since the first enzymatic electrochemical biosensor was reported, but nowadays just a few of them have been commercialized.^{1,2} The main drawback hampering their commercial development is the short-term operational and storage stability.¹ To date, most of the research efforts have been focused on improving the sensitivity and selectivity of the systems. On the other hand, very few publications have successfully addressed the problem of enzyme stability in biosensors. The storage and operational stabilities of an enzymatic electrode are dictated by the retention of the enzyme biological activity.¹ Therefore, the major challenge in the field is to preserve such activity to achieve good repeatability, reproducibility, and prolonged shelf life of the devices. Two main strategies have been explored to address this challenge: (i) substituting the enzymes with (nano)materials

capable to catalyse the same reaction, developing non-enzymatic biosensors,³ (ii) immobilizing the enzymes on solid supports or in selected matrices. The drawback of the first strategy is related to selectivity: although nanomaterials can be efficient catalysts, they will hardly be as selective as enzymes.⁴ The second strategy also presents weaknesses, frequently associated with possible structural changes in the enzyme, caused by immobilization procedures, resulting in loss of the enzyme activity, specificity, or selectivity.^{5,6} For this reason, the choice of the scaffold material and the immobilization strategy are crucial issues to succeed in this task.

Scaffold materials are usually natural polymers (*e.g.*, cellulose, chitosan, agarose, and proteins),^{7–13} synthetic polymers,^{14–16} metallic^{17,18} and polymeric nanoparticles,^{19,20} hydrogels,^{21,22} silica,^{23–25} and metal-organic frameworks.^{26–29}

The sensitivity and overall performance of enzymatic biosensors can be improved tremendously as a result of the incorporation of carbon nanomaterials (CNM) in their fabrication.³⁰ Graphene and carbon nanotubes are attractive materials for the development of amperometric sensors as they allow the direct and efficient electron transfer between enzymes and electrodes.³⁰ However, enzyme immobilization on CNM is challenged by structural perturbations, which can affect their function.^{27,29} In fact, several examples in literature reported low catalytic turnovers and conversion efficiencies for enzymes immobilized onto CNM.^{31,32} To prevent structural perturbation and prolong the enzyme lifespan, CNM and enzymes can be embedded into immobilization matrices, providing a more biologically friendly environment for the biomolecules.^{27,29}

^a Center for Cooperative Research in Biomaterials (CIC BiomaGUNE), Basque Research and Technology Alliance (BRTA), Donostia-San Sebastián, 20014, Spain. E-mail: asilvestri@cicbiomagune.es, alcortajarena@cicbiomagune.es, mprato@cicbiomagune.es

^b Faculty of Chemistry and Food Chemistry and Center for Advancing Electronics Dresden (cfaed), Technische Universität Dresden, Dresden, 01062, Germany

^c Ikerbasque, Basque Foundation for Science, Bilbao, 48009, Spain

^d Department of Chemical and Pharmaceutical Sciences, Università degli Studi di Trieste, Trieste, 34127, Italy

† Electronic supplementary information (ESI) available: TEM, AFM, TGA, Raman, UV-vis, XPS, ζ-potential and electrochemical analyses of EEG materials; SEM micrographs of the electrodes after use; comparison with the literature benchmark. See DOI: 10.1039/d2tc00483f

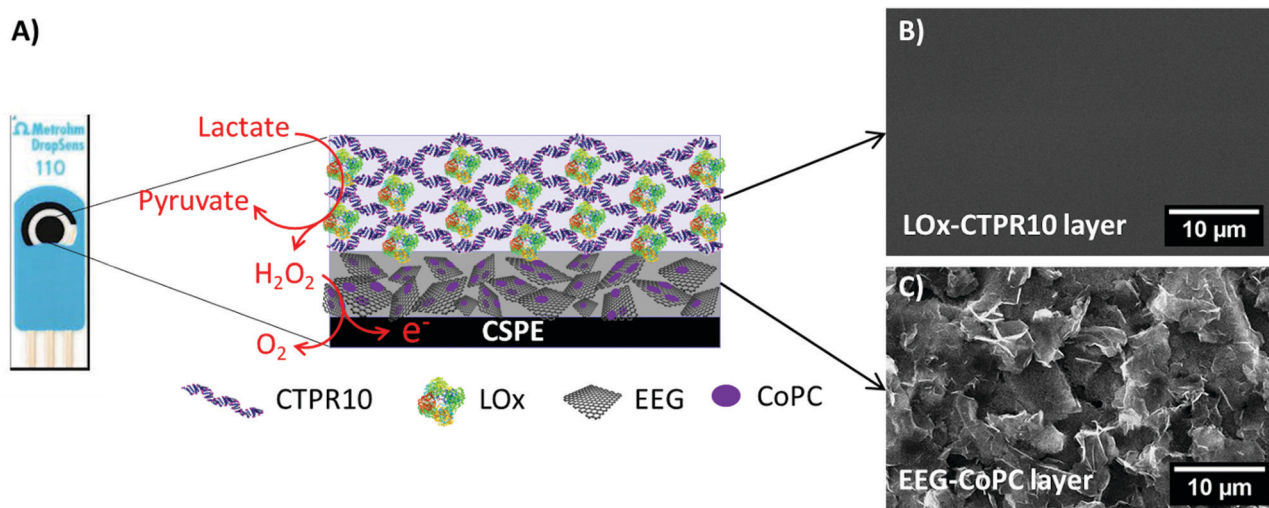


Fig. 1 (A) Design and sensing mechanism of the lactate amperometric biosensor. (B) Scanning electron microscopy (SEM) micrograph of the ordered and homogeneous CTPR10 thin film, containing LOx. (C) SEM micrograph of the electroactive layer of EEG-CoPC.

For example, proteinaceous matrices have been demonstrated to be effective substrates in preserving the enzymatic activity upon immobilization. Previous reports proved that gelatin^{9,33} and bovine serum albumin (BSA)³⁴ can be employed as stabilizing matrices in enzymatic amperometric sensors. Among protein-based materials, self-assembled protein scaffolds are arising as promising immobilization matrices.^{11–13,35–37} Such materials have the advantages of being genetically programmable, produced at relatively low cost by recombinant technology, robust, and able to provide optimal and tuneable microenvironments for catalysis.³⁸ Nevertheless, up to date, these materials have never been used as stabilizing matrices in amperometric biosensors. In the present work, we demonstrate that a particular class of engineered proteins, the consensus tetratricopeptide protein (CTPR), is an outstanding material to immobilize and stabilize enzymes in electrochemical biosensors. CTPR proteins consist of arrays of an identical 34 amino acid consensus sequence.³⁹ Long CTPR proteins, such as CTPR10 composed of 10 repeating units, present a rod-like right-handed super-helical structure,⁴⁰ and can form stable and ordered films due to their side-to-side and head-to-tail interactions.^{41,42} We prove that the integration of CTPR engineered protein film in the sensor design, not only greatly extends the enzyme lifespan (from few days to more than 6 months) but as well improves the repeatability and reproducibility of graphene-based amperometric biosensors. To attest the efficiency of CTPR10 as an enzyme's immobilizing matrix, we designed an amperometric biosensor based on CTPR10, lactate oxidase (LOx), and exfoliated graphene, which enable lactate detection (Fig. 1). LOx was chosen as a model enzyme over glucose oxidase as it is less robust, therefore a more suitable test-bench for our study on activity preservation.^{43–45} Furthermore, lactate is an analyte of primary importance in clinical, sport, toxicological, forensic, and fermentation technologies, being consequently of great economic, and scientific interest.⁴⁶

Experimental

Materials and reagents

Graphite foils were purchased from Alpha Aesar. Reagents and substrates including LOx (*Aerococcus viridans* EU ≥ 20 units mg^{-1}), CoPC, and Lactate were purchased from Sigma Aldrich. Commercial reagents and solvents were used as received, without further purification, unless otherwise stated.

Apparatus and measurements

The prepared materials were characterized by electrochemical techniques, scanning electron microscopy (SEM), transmission electron microscopy (TEM), X-ray photoelectron spectroscopy (XPS), Raman spectroscopy, UV-Vis spectroscopy, atomic force microscopy (AFM), ζ -potential, and thermogravimetric analysis (TGA). Electrochemical characterizations were performed through cyclic voltammetry (CV) and chrono-amperometry (CA), using Autolab MSTAT204 potentiostat/galvanostat (Metrohm) and carbon screen-printed electrodes (C-SPE, DRP110, Metrohm-Dropsens). SEM micrographs were recorded with JEOL JSM-6490LV microscope. The electrodes were sputtered with Au prior to the measurements. TEM micrographs were obtained with a JEOL JEM-1400 PLUS transmission electron microscope equipped with a GATAN US1000 CCD camera, operating at an acceleration voltage of 120 kV. Samples were prepared by drop-casting of EEG isopropanol solutions (0.1 mg mL^{-1}) on ultrathin carbon film-coated Cu-grids (Ted Pella Inc., USA) and dried under ambient conditions. Raman spectra were recorded using a Renishaw Invia Raman spectrometer ($\lambda_{\text{ex}} = 532 \text{ nm}$). Each spectrum is the average of at least 300 spectra recorded in different spots of the sample with 5 s of integration time at a laser power of 1.29 mW. Data were processed using Renishaw WiRE 4 software. XPS measurements were performed in a SPECS Sage HR 100 spectrometer using a nonmonochromatic X-ray source of Mg with a $K\alpha$ line of 1253.6 eV. An electron flood gun was used to avoid sample charging. XPS

samples were prepared drop-casting isopropanol suspensions of the materials on glass slides coated with titanium. XPS data fitting was performed using Casa XPS software (Version 2.3.16 PR 1.6). AFM micrographs were registered using Bruker Multi-mode 8 microscope, employing a tapping mode tip with the frequency of 320 Hz (Bruker TESPA-V2). The samples were prepared by spin coating EEG suspension in isopropanol on freshly cleaved mica. Micrographs were processed using WSxM 5.0 software. The absorbance of the ink was monitored at 660 nm through time-resolved UV-visible spectroscopy, recorded with Beckman Coulter DU 800 spectrophotometer. The ζ -potential measurements were registered using Malvern Nano ZS90 Zetasizer. TGA measurements were performed under N_2 flow (25 mL min^{-1}) using a TGA Discovery (TA Instruments). The samples were equilibrated at $100\text{ }^\circ\text{C}$ for 20 min and then heated from 100 to $800\text{ }^\circ\text{C}$ with a ramp of $10\text{ }^\circ\text{C min}^{-1}$. The data were processed with Trios software (version 3.3.1.4668).

Protein expression and purification

The encoding gene for CTPR10 protein was generated based on a consensus CTPR protein. pPROEX-HTa vector was used to express it as a His-tag fusion for affinity purification.^{47,48} CTPR10 was expressed and purified as described previously.⁴⁷ Briefly, the plasmid was transformed into BL21 (DE3) *Escherichia coli*. Cells were grown in lysogeny broth with 0.1 mg mL^{-1} of ampicillin in agitation until reaching an optical density comprised between 0.6 and 0.8. Then, protein expression was induced by incubating bacteria with 0.6 mM Isopropyl β -D-1-thiogalactopyranoside (IPTG) for 5 hours at $30\text{ }^\circ\text{C}$. Afterward, the cells were centrifuged (4500 rpm) and resuspended in 300 mM NaCl , 50 mM Tris pH = 8.0 Lysis buffer with 1 mg mL^{-1} of lysozyme, $5\text{ mM } \beta$ -mercaptoethanol, and $15\text{ } \mu\text{L}$ DNase stock solution. The obtained lysate was sonicated for 5 minutes with 40% of amplitude and 30 seconds intervals and centrifuged for 45 min at 10 000 rpm. Protein purification was performed by affinity chromatography using Ni^{2+} His-TrapTM column. The eluted protein was dialyzed against PBS (150 mM NaCl , $50\text{ mM phosphate buffer}$ pH = 7.4). The protein was purified and concentrated by fast pressure liquid chromatography (FPLC) (Superdex 75 HiLoad column). Protein fractions were analyzed in 15% acrylamide gels to confirm purity. Finally, the protein was concentrated to 0.55 mM . The protein concentration was estimated using the molar amino acid extinction coefficient at 280 nm calculated from the amino acid sequence.

Electrochemical exfoliation of graphite

Graphene was electrochemically exfoliated by applying an alternating current to a graphite two-electrode system in *N,N*-dimethylformamide (DMF) as previously reported.⁴⁹ Electrochemical exfoliation was followed by tip sonication at $-4\text{ }^\circ\text{C}$ for 30 minutes to control the lateral size of the flakes (22 mm tip , 30% amplitude, 30 min).⁴⁹ The un-exfoliated flakes and large graphene flakes were eliminated by centrifugation (3000 rpm, 10 min).

Synthesis of the 4-carboxyphenyl diazonium tetrafluoroborate

4-Carboxyphenyl diazonium tetrafluoroborate was prepared by dissolving 1 eq. (5 mmol) of 4-aminophenylacetic acid (750 mg, 5 mmol) in a mixture of HBF_4 (2 mL, 32 mmol) and acetic acid (40 mL). A solution of isoamyl nitrate (2 mL, 12 mmol) in acetic acid (20 mL) was added dropwise to the reaction. After 15 min the reaction was quenched with Et_2O (30 mL). The product was purified by crystallization, leaving the reaction mixture overnight at $-22\text{ }^\circ\text{C}$. The precipitate was filtered and washed with ice-cold Et_2O (60 mL). $^1\text{H-NMR}$ (400 MHz, MeOD, δ): 8.49 (d, 2H, Ar H), 7.85 (d, 2H, Ar H), 3.91 (s, 2H, CH_2). IR (KBr): $\nu = 2297\text{ cm}^{-1}$ (s; $\nu(N\equiv N)$).

Synthesis of the EEG-CoPC electroactive ink

EEG-CoPC was synthesized accordingly to the previously reported procedure.⁴⁹ Briefly, 4-carboxyphenyl diazonium tetrafluoroborate (500 mg) was added to a dispersion of EEG in DMF (50 mg mL^{-1}). The reaction was stirred overnight at $80\text{ }^\circ\text{C}$. The product was filtered using $0.1\text{ } \mu\text{m}$ PTFE membranes. The EEG-COOH was washed with the following solvents DMF (2 \times), AcOEt (2 \times), MeOH (2 \times), Acetone (2 \times), Et_2O (1 \times). The residues of solvents were removed at reduced pressure. The obtained functionalized EEG was suspended in DMF (50 mL) and incubated with 10% of CoPC (5 mg) for 12 h at room temperature (RT) under constant stirring. The obtained EEG-CoPC was purified by filtration over $0.1\text{ } \mu\text{m}$ PTFE membranes and washed with DMF until no CoPC was present in the recovered solvent. The electroactive ink was suspended in ultrapure water.

Biosensor manufacturing

Firstly, $5.0\text{ } \mu\text{L}$ of the EEG-CoPC electroactive ink (1.0 mg mL^{-1}) was spin-coated over the working electrode of a CSPE (time = 30 s, speed = 2500 rpm, acceleration = 770 rpm s^{-1}). Subsequently, $5.0\text{ } \mu\text{L}$ of a homogeneous mixture of CTPR10 protein (0.55 mM) and LOx (0.03 mM) was spin-coated over the first layer. Finally, a layer of Nafion was drop casted ($2\text{ } \mu\text{L}$, 1%, neutralized at pH 7) atop to avoid mechanical detachment of the nanomaterials during FIA analyses.

Electrochemical measurements

CV was performed in the range of potential from -0.1 V to $+0.5\text{ V}$ at a scan rate of 20 mV s^{-1} . Phosphate buffer (0.1 mM at pH 7) enriched with 0.1 mM of KCl was used as an electrolyte. The amperometric detection was performed using a flow injection analysis (FIA) setup: a flow cell (Metrohm-Dropsens) coupled with an HPLC injection valve (100 mL) and a peristaltic pump. Freshly prepared lactate solutions were injected in a continuous flow of the electrolyte (1.0 mL min^{-1}). For each concentration level, three consecutive injections were performed. For the CA analysis in human serum (HS), 10 times diluted human serum (Sigma Aldrich) enriched with 0.01 mM of KCl was employed as an electrolyte medium. Lactate solutions at different concentrations were freshly prepared in human serum enriched with 0.1 mM of KCl and diluted 10 times prior to injection. The solutions at known

concentrations were introduced in a continuous electrolyte flow stream (1.0 mL min^{-1}). The calibration plots for the different systems were obtained by plotting the obtained current intensity against the analyte concentration. Sensitivity was calculated from the slope in the linear range and normalized to the electrode area. The noise was calculated as the standard deviation of the current signal in absence of analyte (baseline)-sampled for a period of at least 20 seconds. The limit of detection (LOD) was calculated as three times the standard deviation of the baseline. The repeatability was assessed by performing three consecutive calibrations on the same electrode. The reproducibility was assessed by performing calibration on three different electrodes during the same day. The storage stability was assessed by performing calibrations at different time points over 6 months. At each time point, the calibration was performed in triplicates.

Results and discussion

In the present work, an amperometric biosensor for lactate detection is developed, by modifying the working electrode of commercial CSPE with a double layer (Fig. 1A). In the bottom layer, a conductive and electrocatalytic water-based ink is deposited over the CSPE by spin coating (Fig. 1C). Such ink is composed of electrochemically exfoliated graphene (Fig. S1–S3, ESI†), functionalized with phenylacetic acid moieties and CoPC (Fig. S4, ESI†). The phenylacetic acid moieties are introduced by reaction of EEG with phenylacetic acid diazonium salts and provide electrostatic stability to the flake (Fig. S5 and S6, ESI†).⁴⁹ CoPC is adsorbed over the basal plane of EEG through stable π - π interactions and works as an electrochemical mediator for H_2O_2 oxidation. Further details on the manufacture and characterization of this electroactive ink are reported in ESI† and in previous publications of the group (Fig. S7–S10, ESI†).⁴⁹ On top of the first layer, a second one is deposited by spin coating, containing a homogeneous mixture of LOx, the receptor of the biosensor, and CTPR10 protein, used as an immobilizing and stabilizing agent for the enzyme. Upon solvent evaporation, the CTPR10 units self-assemble through side-to-side and head-to-tail interactions, forming a thin and ordered protein film that physically entraps LOx (Fig. 1B), as previously demonstrated for other enzymes.¹¹

The biosensor works as follows: LOx catalyses the oxidation of lactate present in the solution into pyruvate. During the process, H_2O_2 is produced and diffuses through the protein film until it reaches the electrocatalytic EEG-CoPC layer, where its oxidation is mediated by CoPC. The electrons produced during H_2O_2 oxidation are efficiently transferred to the electrode through EEG, thanks to the elevated conductivity of the material (Fig. 1A). Furthermore, the EEG deposited over the electrode forms a nanostructured surface (Fig. 1C), increasing the active surface area of the electrode.

To assess the permeability of the CTPR10 film to small electroactive species, CV was performed in a solution of potassium hexacyanoferrate(II) in phosphate buffer saline solution

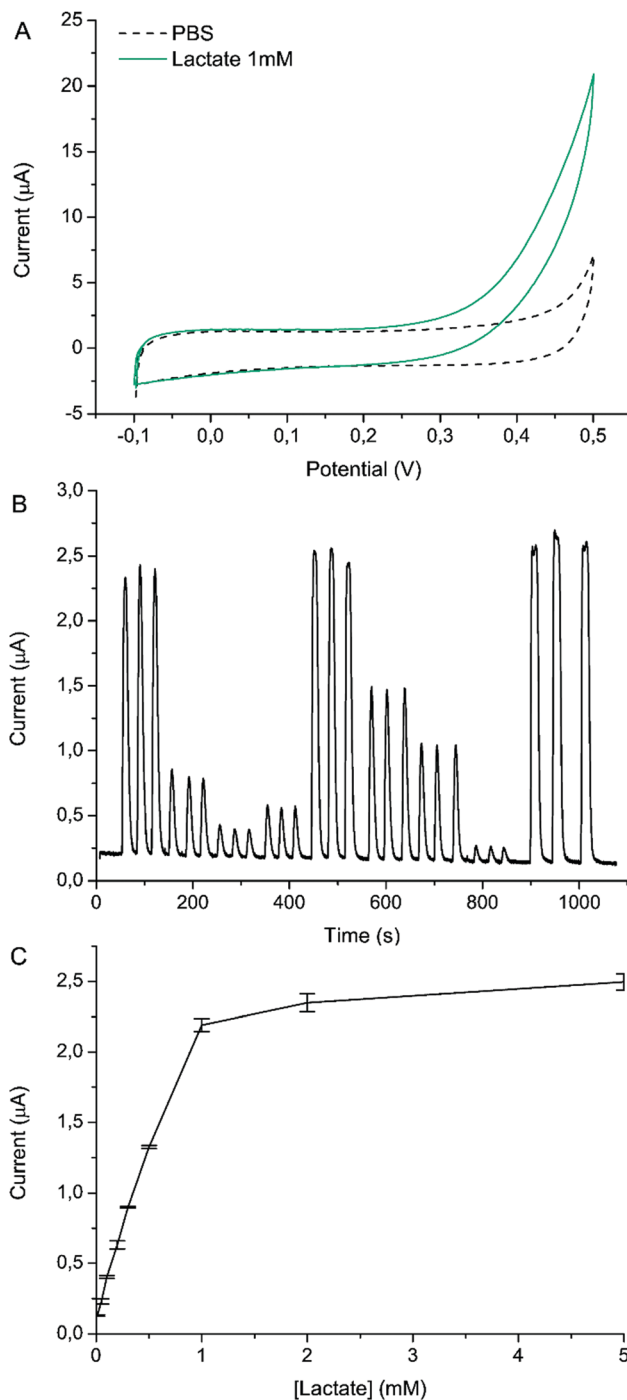


Fig. 2 Electrochemical sensing of lactate concentration in PBS. (A) CV responses obtained with CSPE/EEG-CoPC/LOx-CTPR10, in the absence (dashed line) and in the presence (solid line) of 1 mM of lactate (scan rate 20 mV s^{-1}). (B) FIA response obtained from CSPE/EEG-CoPC/LOx-CTPR10. Nine different lactate concentrations were tested, namely 0.01, 0.05, 0.1, 0.2, 0.3, 0.5, 1, 2, and 5 mM. ($E = +0.4 \text{ V}$, flow rate = 1 mL min^{-1}). (C) Trend of the current measured in FIA vs. lactate concentration. The linear regime was found between 0.01 and 1 mM. Error bars represent the standard deviation among three injections in the same analysis.

(PBS), in the absence and the presence of the protein thin film. When the CTPR10 film was deposited onto the electrode, the

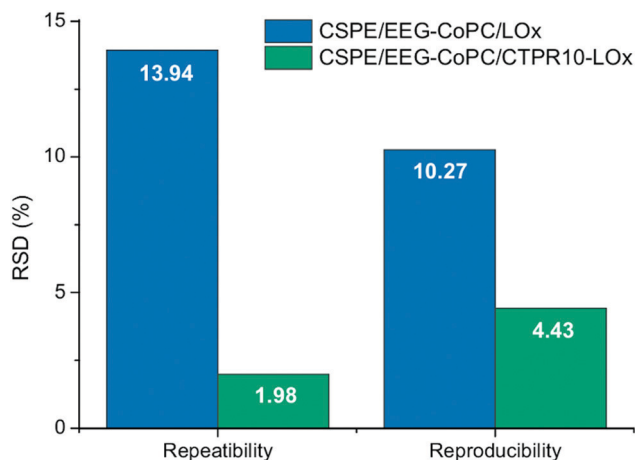


Fig. 3 Repeatability and reproducibility RSD% values obtained for LOX-CTPR10/EEG-CoPC and LOX/EEG-CoPC (control).

redox peaks of the electrochemical mediator were still visible but showed reduced current intensity, when compared to the naked electrode (Fig. S11, ESI†). Such evidence suggested that the protein film shields the electrode surface, but still allows the diffusion of the mediator. Another critical point, for the applicability of CTPR10 films in electro-analytical devices, is that the protein film should not be affected by the application of a potential. To verify the stability of the protein under working conditions, CV of the electrode modified with the thin film was performed in PBS in the range from -0.1 to 0.5 V. No redox peak was detected, confirming that CTPR10 did not undergo reduction or oxidation reactions in the selected window of potential (Fig. S12, ESI†).

The applicability of LOX-CTPR10/EEG-CoPC modified CSPE in sensing lactate was investigated by means of electrochemical methods. Fig. 2A reports the CV recorded after incubating the modified electrode in phosphate buffer saline (PBS), in the absence (blank), and in the presence of 1.0 mM lactate. In the

presence of lactate, an intense current increase was registered at potentials higher than $+0.25$ V, which could be ascribed to H_2O_2 oxidation, catalysed by CoPC. Amperometric measurements at a fixed potential of $+0.4$ V were performed using a flow injection analysis (FIA) setup, to evaluate the lactate concentration-dependent response. Ten different concentrations of lactate (from 0.01 to 5 mM, run in triplicates) were injected in a PBS flow-stream passing over the electrode (Fig. 2B). The baseline was found to be flat, free of drifting, and characterized by an extremely low noise (5.31 nA). No variability was observed among the three consecutive injections performed for each concentration, proving the reliable response of the setup. The sensitivity of the biosensor was $17.66 \mu\text{A cm}^{-2} \text{ mM}^{-1}$, with a limit of detection (LOD) of $1.24 \mu\text{M}$ and a limit of quantification (LOQ) of $4.12 \mu\text{M}$. The biosensors had a linear response against lactate concentration, in the range of 1 – $1000 \mu\text{M}$ (Fig. 2C). SEM images of the electrode surface were taken before and after the amperometric measurement, confirming that the CTPR10 film was still present after the use, even if affected by a slight deterioration (Fig. S13, ESI†).

To evaluate the effect of the CTPR10 thin film on the sensor performance, control electrodes were manufactured by spin coating in the order EEG-CoPC and LOx (without CTPR10) onto CSPE. The CSPE/EEG-CoPC/LOX-CTPR10 and the CSPE/EEG-CoPC/LOx control electrodes were tested in terms of repeatability, reproducibility, and storage stability. Repeatability and reproducibility were evaluated at day one. Repeatability was assessed by performing three consecutive calibrations over the same CSPE, while reproducibility was calculated from the calibrations of three different electrodes. Both the parameters are expressed as the relative standard deviation (RSD%) among the slopes of the triplicates. Due to the presence of CTPR10 film, the RSD values related to repeatability were reduced from 13.94% (for LOX/EEG-CoPC, control experiment) to 1.98% (for LOX-CTPR10/EEG-CoPC, Fig. 3 and Fig. S14, ESI†). The reduced variability among consecutive measurements testifies that the protein film improves the operational stability of the devices. As well, the reproducibility of the measurements improved by

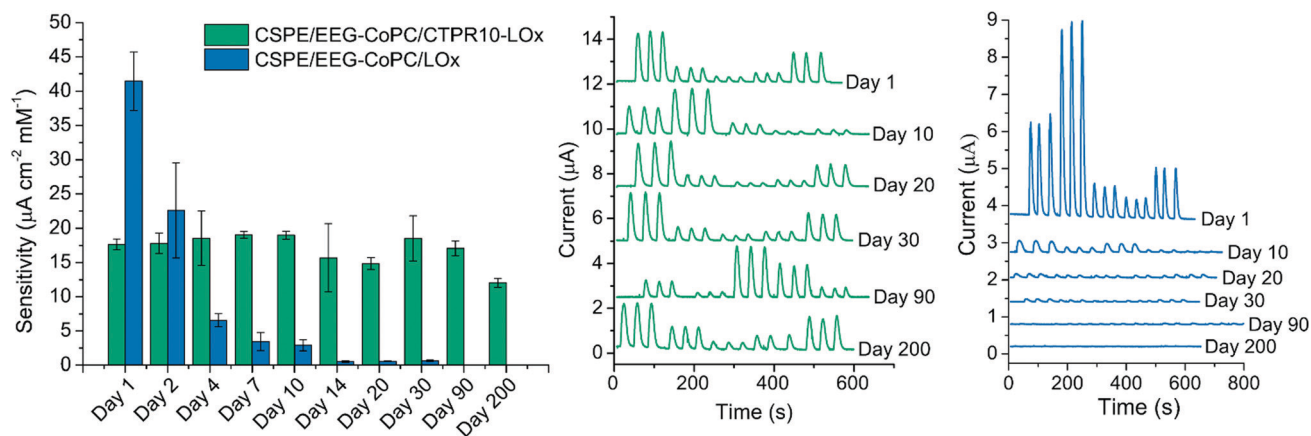


Fig. 4 (A) Sensitivity of LOX-CTPR10/EEG-CoPC and LOX/EEG-CoPC (control) monitored for 200 days. (B) Representative FIAs of LOX-CTPR10/EEG-CoPC at different time points. (C) Representative FIAs of LOX/EEG-CoPC (control) at different time points.

the incorporation of the CTPR10 thin film, as indicated by the reduction of the RSD values from 10.27% (for LOX/EEG-CoPC) to 4.43% (for LOX-CTPR10/EEG-CoPC, Fig. 3 and Fig. S14, ESI†).

The most evident benefit deriving from the use of CTPR10 is the extension of the storage stability of the devices. The sensitivity of both LOX-CTPR10/EEG-CoPC and LOX/EEG-CoPC (control experiment) was monitored at different time points over the course of six months at RT (Fig. 4A). At each time point, the sensitivities of three LOX-CTPR10/EEG-CoPC and three control electrodes were evaluated through chrono-amperometric titration (Fig. 4B). When CTPR10 thin films were used, the sensitivity of the devices was maintained unaffected for 90 days and reduced to 70% after more than 6 months, while, in the control, the enzymatic activity was rapidly lost as indicated from the dramatic sensitivity decrease. Furthermore, the preservation of enzymatic activity at RT, due to the presence of the CTPR10 film, is an outstanding result that can simplify the electrode storage, avoiding the costly cold chain preservation. In previous investigations, protein-based biomaterials were demonstrated to be effective in immobilizing enzymes and preserving their catalytic activity.^{9,33,34,38} As shown in the present work, the engineered CTPR10 makes no exception, stabilizing lactate oxidase for several months at RT. A further advantage of CTPR as stabilizing matrix is that these designed proteins are strikingly stable when compared to natural proteins,⁵⁰ resulting in more robust materials. In addition, they can be engineered and modified to modulate their properties including their stability,⁵¹ or to add extra functions such as catalytic activities or additional functional nanomaterials.⁵²

The extraordinary stabilizing properties of CTPR proteins could derive from the combination of several factors, namely: (i) avoiding the disruption of the enzyme native conformation upon dehydration;⁵³ (ii) preventing enzyme aggregation during the drying process;⁵³ (iii) providing a patched hydrophobic/hydrophilic surface with domains analogous to the ones of enzymes;¹⁵ and (iv) having an optimal pH micro-environment and superficial charge distribution.⁵⁴ All together these factors provide a favourable environment for enzymes, closely resembling their native conditions in highly crowded cellular environments.

We compared the performances of the herein presented LOX-based biosensor, with the literature benchmark (Table S1, ESI†). LOX-CTPR10/EEG-CoPC CPSE presents extremely prolonged storage stability at RT, which can be found only in a few examples in the literature.^{9,55,56} Moreover, our design presents a good compromise among prolonged storage stability, elevated sensitivity, reduced LOD, and fast time of response, making it an extremely competitive biosensor.

To assess the applicability of the ink in complex biological matrices, CV and amperometric analysis were performed in human serum (HS, Fig. 5). The concentration of blood lactate is usually comprised between 1–2 mmol L⁻¹ at rest and can rise to concentrations greater than 20 mmol L⁻¹ during intense physical exercise.⁵⁷ Therefore, to centre the linear range of the sensor we first spiked HS samples with lactate and then diluted

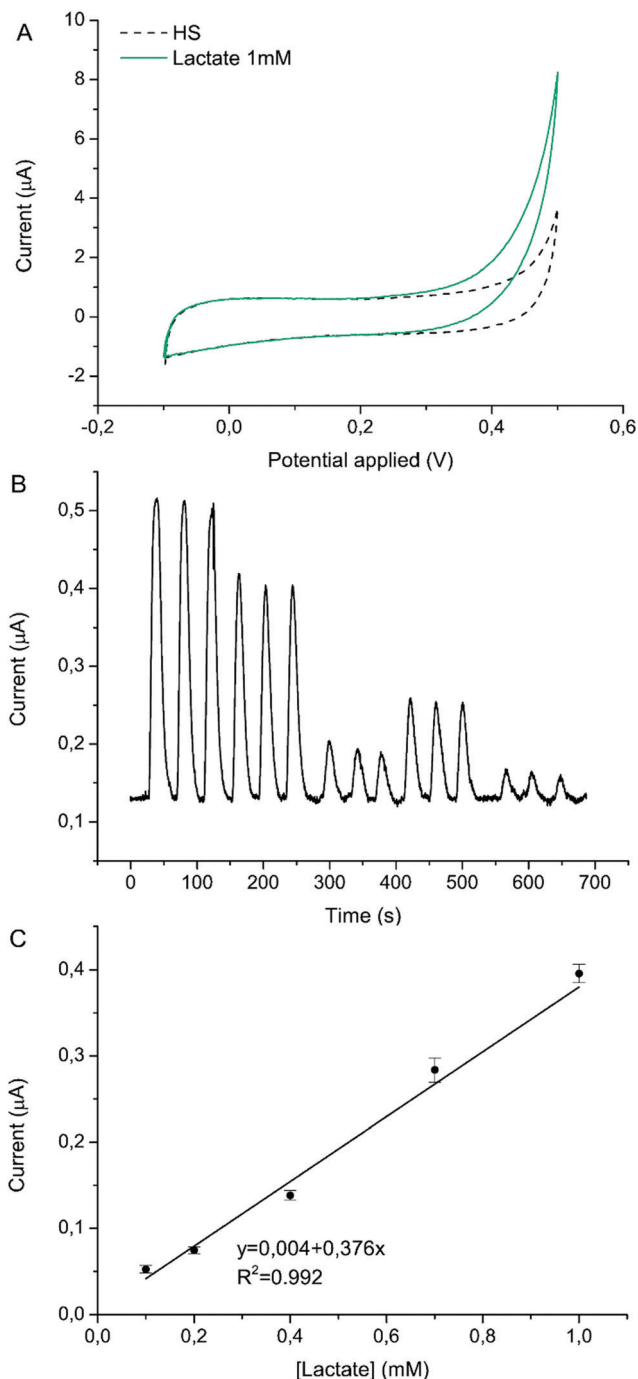


Fig. 5 Electrochemical sensing of lactate concentration in HS. (A) CV responses obtained with CSPE/EEG-CoPC/LOX-CTPR10, in the absence (dashed line) and in the presence (solid line) of 1 mM of lactate (scan rate 20 mV s⁻¹). (B) FIA response obtained from CSPE/EEG-CoPC/LOX-CTPR10. Five different lactate concentrations were tested, namely 0.1, 0.2, 0.4, 0.7, and 1 mM. ($E = +0.4$ V, flow rate = 1 mL min⁻¹). (C) Trend of the current measured in FIA vs. lactate concentration. The linear regime was found between 0.1 and 1 mM. Error bars represent the standard deviation among three injections in the same analysis.

them 10 times. The final lactate concentrations tested were of 0.1, 0.2, 0.4, 0.7, and 1 mM. FIA amperometric measurements show that the stable and flat baseline is preserved in HS as well

as the fast response time of the sensor. The sensitivity obtained in HS is lower than in PBS ($3.75 \mu\text{A cm}^{-2} \text{mM}^{-1}$) but still allows to reach low LOD ($3.1 \mu\text{M}$). The linear range did not change with respect to that obtained in PBS.

Conclusions

In the present paper, we demonstrated that thin films composed of engineered repeat proteins (CTPR10) are an extraordinary proteinaceous immobilizing and stabilizing agent for enzymes such as LOx. Moreover, we demonstrated that such biomaterial can be successfully incorporated into the design of amperometric enzymatic biosensors. The resulting devices are characterized by elevated sensitivity and reduced LOD, provided by the presence of EEG-CoPC, which works as an efficient transducer. Furthermore, the presence of CTPR10 protein films strongly improves both the storage and the operational stability, reducing the RSD relative to repeatability and reproducibility of one order of magnitude. The combination of the two materials furnishes a biosensor with a perfect balance between stability and sensitivity.

Author contributions

Alessandro Silvestri: Conceptualization, data curation, formal analysis, investigation, methodology, project administration, supervision, writing – original draft, writing – review & editing. Faxing Wang: investigation, methodology, writing – review & editing. Xinliang Feng: supervision, writing – review & editing. Aitziber L. Cortajarena: conceptualization, project administration, supervision, writing – review & editing. Maurizio Prato: conceptualization, project administration, supervision, writing – review & editing.

Conflicts of interest

The authors declare that they have no known competing financial interests or personal relationships that could have appeared to influence the work reported in this paper.

Acknowledgements

A. S. thanks Grant FJC2018-036777-I funded by MCIN/AEI/10.13039/501100011033. M. P., as the recipient of the AXA Bionanotechnology Chair, is grateful to the AXA Research Fund for financial support. A. L. C. acknowledges Grant PID2019-111649RB-I00 funded by MCIN/AEI/10.13039/501100011033, and Grant PDC2021-120957-I00 funded by MCIN/AEI/10.13039/501100011033 and by the “European Union NextGenerationEU/PRTR”. This work was performed under the Grant MDM-2017-0720 funded by MCIN/AEI/10.13039/501100011033.

Notes and references

- 1 J. I. Reyes-De-Corcuera, H. E. Olstad and R. García-Torres, *Annu. Rev. Food Sci. Technol.*, 2018, **9**, 293–322.
- 2 L. C. Clark Jr. and C. Lyons, *Ann. N. Y. Acad. Sci.*, 1962, **102**, 29–45.
- 3 Y. Huang, J. Ren and X. Qu, *Chem. Rev.*, 2019, **119**, 4357–4412.
- 4 J. J. Gooding, *ACS Sens.*, 2019, **4**, 2213–2214.
- 5 A. Sassolas, L. J. Blum and B. D. Leca-Bouvier, *Biotechnol. Adv.*, 2012, **30**, 489–511.
- 6 R. C. Rodrigues, C. Ortiz, Á. Berenguer-Murcia, R. Torres and R. Fernández-Lafuente, *Chem. Soc. Rev.*, 2013, **42**, 6290–6307.
- 7 S. Martins de Oliveira, S. Velasco-Lozano, A. H. Orrego, J. Rocha-Martín, S. Moreno-Pérez, J. M. Fraile, F. López-Gallego and J. M. Guisán, *Biomacromolecules*, 2021, **22**, 927–937.
- 8 W.-C. Huang, W. Wang, C. Xue and X. Mao, *ACS Sustainable Chem. Eng.*, 2018, **6**, 8118–8124.
- 9 G. F. Khan and W. Wernet, *Anal. Chem.*, 1997, **69**, 2682–2687.
- 10 Y. Liu, Z. Cai, Y. Jin, L. Sheng and M. Ma, *ACS Sustainable Chem. Eng.*, 2020, **8**, 15560–15572.
- 11 D. Sánchez-deAlcázar, S. Velasco-Lozano, N. Zeballos, F. López-Gallego and A. L. Cortajarena, *ChemBioChem*, 2019, **20**, 1977–1985.
- 12 G. Zhang, T. Johnston, M. B. Quin and C. Schmidt-Dannert, *ACS Synth. Biol.*, 2019, **8**, 1867–1876.
- 13 G. Zhang, M. B. Quin and C. Schmidt-Dannert, *ACS Catal.*, 2018, **8**, 5611–5620.
- 14 E. M. Pelegri-O'Day, S. J. Paluck and H. D. Maynard, *J. Am. Chem. Soc.*, 2017, **139**, 1145–1154.
- 15 B. Panganiban, B. Qiao, T. Jiang, C. DelRe, M. M. Obadia, T. D. Nguyen, A. A. A. Smith, A. Hall, I. Sit1, M. G. Crosby, P. B. Dennis, E. Drockenmuller, M. Olvera de la Cruz and T. Xu, *Science*, 2018, **359**, 1239–1243.
- 16 J. Ye, T. Chu, J. Chu, B. Gao and B. He, *ACS Sustainable Chem. Eng.*, 2019, **7**, 18048–18054.
- 17 H. R. de Barros, I. García, C. Kuttner, N. Zeballos, P. H. C. Camargo, S. I. C. de Torresi, F. López-Gallego and L. M. Liz-Marzán, *ACS Catal.*, 2021, **11**, 414–423.
- 18 K. Szekeres, P. Bollella, Y. Kim, S. Minko, A. Melman and E. Katz, *J. Phys. Chem. Lett.*, 2021, **12**, 2523–2527.
- 19 D. Keller, A. Beloqui, M. Martínez-Martínez, M. Ferrer and G. Delaittre, *Biomacromolecules*, 2017, **18**, 2777–2788.
- 20 D. Wang and W. Jiang, *Int. J. Biol. Macromolecules*, 2019, **126**, 1125–1132.
- 21 M. P. Conte, K. H. A. Lau and R. Ulijn, *ACS Appl. Mater. Interfaces*, 2017, **9**, 3266–3271.
- 22 A. Beloqui, A. Y. Kobitski, G. U. Nienhaus and G. Delaittre, *Chem. Sci.*, 2018, **9**, 1006–1013.
- 23 S. Kim, K. Joo, B. H. Jo and H. J. Cha, *ACS Appl. Mater. Interfaces*, 2020, **12**, 27055–27063.
- 24 T. Zhai, C. Wang, F. Gu, Z. Meng, W. Liu and Y. Wang, *ACS Sustainable Chem. Eng.*, 2020, **8**, 15250–15257.

- 25 Y. Zhang, Q. Yue, M. M. Zagho, J. Zhang, A. A. Elzatahry, Y. Jiang and Y. Deng, *ACS Appl. Mater. Interfaces*, 2019, **11**, 10356–10363.
- 26 Y. Pan, H. Li, J. Farmakes, F. Xiao, B. Chen, S. Ma and Z. Yang, *J. Am. Chem. Soc.*, 2018, **140**, 16032–16036.
- 27 S. Neupane, K. Patnode, H. Li, K. Baryeh, G. Liu, J. Hu, B. Chen, Y. Pan and Z. Yang, *ACS Appl. Mater. Interfaces*, 2019, **11**, 12133–12141.
- 28 T. H. Wei, S. H. Wu, Y. D. Huang, W. S. Lo, B. P. Williams, S. Y. Chen, H. C. Yang, Y. S. Hsu, Z. Y. Lin, X. H. Chen, P. E. Kuo, L. Y. Chou, C. K. Tsung and F. K. Shieh, *Nat. Commun.*, 2019, **10**, 5002.
- 29 J. Farmakes, I. Schuster, A. Overby, L. Alhalhooly, M. Lenertz, Q. Li, A. Ugrinov, Y. Choi, Y. Pan and Z. Yang, *ACS Appl. Mater. Interfaces*, 2020, **12**, 23119–23126.
- 30 Y. Shao, J. Wang, H. Wu, J. Liu, I. A. Aksay and Y. Lin, *Electroanalysis*, 2010, **22**, 1027–1036.
- 31 H. Seelajaroen, A. Bakandritsos, M. Otyepka, R. Zbořil and N. S. Sariciftci, *ACS Appl. Mater. Interfaces*, 2020, **12**, 250–259.
- 32 J. Zhang, F. Zhang, H. Yang, X. Huang, H. Liu, J. Zhang and S. Guo, *Langmuir*, 2010, **26**, 6083–6085.
- 33 Y. Wang, T. Li, W. Zhang and Y. Huang, *J. Solid State Electrochem.*, 2014, **18**, 1981–1987.
- 34 C. He, M. Xie, F. Hong, X. Chai, H. Mi, X. Zhou, L. Fan, Q. Zhang, T. Ngai and J. Liu, *Electrochim. Acta*, 2016, **222**, 1709–1715.
- 35 S. Lim, G. A. Jung, D. J. Glover and D. S. Clark, *Small*, 2019, **15**, 1805558.
- 36 S. A. McConnell, K. A. Cannon, C. Morgan, R. McAllister, B. R. Amer, R. T. Clubb and T. O. Yeates, *ACS Synth. Biol.*, 2020, **9**, 381–391.
- 37 A. Rodríguez-Abetxuko, D. Sánchez-deAlcázar, P. Muñumer and A. Beloqui, *Front. Bioeng. Biotechnol.*, 2020, **8**, 830.
- 38 J. M. Guisan, F. López-Gallego, J. M. Bolivar, J. Rocha-Martín and G. Fernandez-Lorente, in *Immobilization of Enzymes and Cells: Methods and Protocols*, ed. J. M. Guisan, J. M. Bolivar, F. López-Gallego and J. Rocha-Martín, Springer US, New York, NY, 2020, pp. 1–26.
- 39 E. R. G. Main, Y. Xiong, M. J. Cocco, L. D'Andrea and L. Regan, *Structure*, 2003, **11**, 497–508.
- 40 T. Kajander, A. L. Cortajarena, S. Mochrie and L. Regan, *Acta Crystallogr., Sect. D: Biol. Crystallogr.*, 2007, **63**, 800–811.
- 41 T. Z. Grove, L. Regan and A. L. Cortajarena, *J. R. Soc., Interface*, 2013, **10**, 20130051.
- 42 D. Sanchez-deAlcazar, D. Romera, J. Castro-Smirnov, A. Sousaraei, S. Casado, A. Espasa, M. C. Morant-Miñana, J. J. Hernandez, I. Rodríguez, R. D. Costa, J. Cabanillas-Gonzalez, R. V. Martinez and A. L. Cortajarena, *Nanoscale Adv.*, 2019, **1**, 3980–3991.
- 43 H. Minagawa, N. Nakayama, T. Matsumoto and N. Ito, *Biosens. Bioelectron.*, 1998, **13**, 313–318.
- 44 H. Minagawa, Y. Yoshida, N. Kenmochi, M. Furuichi, J. Shimada and H. Kaneko, *Cell. Mol. Life Sci.*, 2007, **64**, 77–81.
- 45 B. Lillis, C. Grogan, H. Berney and W. A. Lane, *Sens. Actuators, B*, 2000, **68**, 109–114.
- 46 G. Rattu, N. Khansili, V. Kumar and M. Prayaga, *Environ. Chem. Lett.*, 2021, **19**, 1135–1152.
- 47 T. Kajander, A. L. Cortajarena, E. R. G. Main, S. G. J. Mochrie and L. Regan, *J. Am. Chem. Soc.*, 2005, **127**, 10188–10190.
- 48 T. Kajander, A. L. Cortajarena and L. Regan, in *Protein Design: Methods and Applications*, ed. R. Guerois and M. L. de la Paz, Humana Press, Totowa, NJ, 2006, pp. 151–170.
- 49 A. Silvestri, A. Criado, F. Poletti, F. Wang, P. Fanjul-Bolado, M. B. González-García, C. García-Astrain, L. M. Liz-Marzán, X. Feng, C. Zanardi and M. Prato, *Adv. Funct. Mater.*, 2021, **32**, 2105028.
- 50 A. L. Cortajarena and L. Regan, *Protein Sci.*, 2011, **20**, 336–340.
- 51 A. L. Cortajarena, S. G. J. Mochrie and L. Regan, *Protein Sci.*, 2011, **20**, 1042–1047.
- 52 A. Aires, I. Llarena, M. Moller, J. Castro-Smirnov, J. Cabanillas-Gonzalez and A. L. Cortajarena, *Angew. Chem., Int. Ed.*, 2019, **58**, 6214–6219.
- 53 T. Shimizu, T. Korehisa, H. Imanaka, N. Ishida and K. Imamura, *Biosci., Biotechnol., Biochem.*, 2017, **81**, 687–697.
- 54 Y. Zhang, S. Tsitkov and H. Hess, *Nat. Commun.*, 2016, **7**, 13982.
- 55 Q. Yang, P. Atanasov and E. Wilkins, *Biosens. Bioelectron.*, 1999, **14**, 203–210.
- 56 R. Monošík, M. Středanský, G. Greif and E. Šturdík, *Food Control*, 2012, **23**, 238–244.
- 57 K. Rathee, V. Dhull, R. Dhull and S. Singh, *Biochem. Biophys. Rep.*, 2016, **5**, 35–54.